Behavioral/Systems/Cognitive

Homeostatic Synapse-Driven Membrane Plasticity in Nucleus Accumbens Neurons

Masago Ishikawa,[1,2] Ping Mu,[1,2] Jason T. Moyer,[4] John A. Wolf,[5] Raymond M. Quock,[3] Neal M. Davies,[3] Xiu-ti Hu,[6] Oliver M. Schlüter,[7] and Yan Dong[1,2]

[1]Program in Neuroscience and Departments of [2]Veterinary and Comparative Anatomy, Pharmacology, and Physiology and [3]Pharmaceutical Sciences, Washington State University, Pullman, Washington 99164-6520, Departments of [4]Bioengineering and [5]Neuroscience, University of Pennsylvania, Philadelphia, Pennsylvania 19104, [6]Department of Pharmacology, Rush University, Chicago, Illinois 60612, and [7]Department of Molecular Neurobiology, European Neuroscience Institute, 37077 Göttingen, Germany

Stable brain function relies on homeostatic maintenance of the functional output of individual neurons. In general, neurons function by converting synaptic input to output as action potential firing. To determine homeostatic mechanisms that balance this input–output/synapse–membrane interaction, we focused on nucleus accumbens (NAc) neurons and demonstrated a novel form of synapse-to-membrane homeostatic regulation, homeostatic synapse-driven membrane plasticity (*h*SMP). Through *h*SMP, NAc neurons adjusted their membrane excitability to functionally compensate for basal shifts in excitatory synaptic input. Furthermore, *h*SMP was triggered by synaptic NMDA receptors (NMDARs) and expressed by the modification of SK-type Ca^{2+}-activated potassium channels. Moreover, *h*SMP in NAc neurons was abolished in rats during a short- (2 d) or long- (21 d) term withdrawal from repeated intraperitoneal injections of cocaine (15 mg/kg/d, 5 d). These results suggest that *h*SMP is a novel form of synapse-to-membrane homeostatic plasticity and dysregulation of *h*SMP may contribute to cocaine-induced cellular alterations in the NAc.

Introduction

Homeostatic plasticity is an important cellular mechanism through which neurons use the neuroplasticity machinery to maintain stable functional output in an ever-changing internal and external environment (Turrigiano and Nelson, 2004). The functional output of a neuron relies on dynamic integration of synaptic inputs and intrinsic membrane excitability. It has long been known that homeostatic plasticity can occur independently at either synapses (Turrigiano and Nelson, 2004) or the membrane excitability (Zhang and Linden, 2003). For example, synaptic transmission debilitated by decreased presynaptic release tends to be compensated by a homeostatic scaling-up of the postsynaptic responsiveness, whereas a decrease in the intrinsic membrane excitability by inhibition of Na^+ channels can be ameliorated or compensated by regulating a set of ion channels to increase the membrane excitability (Desai et al., 1999; Davis, 2006). Poorly understood are the homeostatic mechanisms that coordinate the synaptic activity and membrane excitability such that the integration of synapse–membrane interaction is stabilized. Recent findings demonstrate that inhibition of action potential firing induces a rapid homeostatic increase in excitatory synaptic strength, indicating that a homeostatic membrane-to-synapse regulation may exist in mammalian neurons (Ibata et al., 2008). In the current study, we ask: does synapse-to-membrane homeostatic regulation exist?

It has been shown that membrane excitability can be modulated by synaptic signaling in an experience-dependent manner (Aizenman and Linden, 2000; Egorov et al., 2002; Sourdet et al., 2003; Xu and Kang, 2005), suggesting that modulatory intracellular signaling does exist from synapses to cell membranes. To identify the homeostatic synapse-to-membrane regulation, we focused on nucleus accumbens (NAc) medium spiny neurons (MSNs), whose output critically relies on a fine balance between excitatory synaptic input and membrane excitability (O'Donnell and Grace, 1995; Plenz and Kitai, 1998; O'Donnell et al., 1999). Our results show that the intrinsic membrane excitability of NAc MSNs could be gradually increased or decreased in response to a persistent decrease or increase in the basal excitatory synaptic activities. This compensatory synapse-to-membrane modulation tended to maintain the overall functional state of neurons and was thus termed homeostatic synapse-driven membrane plasticity (*h*SMP). Furthermore, *h*SMP in NAc MSNs was initiated by NMDA receptors (NMDARs), expressed by modification of SK type Ca^{2+}-activated potassium channels, and abolished in rats pretreated with cocaine. Together, these results indicate that identification of *h*SMP may provide a novel angle in understanding drug-induced cellular and functional alterations of NAc neurons.

Received Nov. 30, 2008; revised April 8, 2009; accepted April 8, 2009.

This research was supported in part by State of Washington Initiative Measure 171, National Institutes of Health (NIH) DA023206, and the Hope Foundation for Depression Research. Cocaine was supplied in part by the Drug Supply Program of NIH–National Institute on Drug Abuse. The European Neuroscience Institute Göttingen is jointly funded by the Göttingen University Medical School and the Max Planck Society. This work was also suppported by the German Science Foundation (SCHL 592/4-1 to O.M.S.), the Göttingen University Medical School, the Max Planck Society, and the European Commission Coordination Action ENINET (contract number LSHM-CT-2005-19063). We thank Drs. Yanhua Huang, Yavin Shaham, and Brian Lee for suggestions on experimental design and manuscript organization, and Dr. Bryan Slinker for expert statistical analysis suggestions.

Correspondence should be addressed to Dr. Yan Dong or Dr. Oliver Schlüter, Wegner 205, PO Box 646520, Washington State University, Pullman, WA 99164-6520, E-mail: yan_dong@wsu.edu or oschlue@gwdg.de.

DOI:10.1523/JNEUROSCI.5703-08.2009

 0270-6474/09/295820-12$15.00/0

Materials and Methods

Animal use and intraperitoneal injection of cocaine. Thirty-two- to sixty-day-old male Sprague Dawley rats were used for all experiments. Before drug administration or molecular manipulation, rats were allowed to acclimate to their home cages for >5 d. For cocaine treatment, we used a 5 d cocaine procedure, which was similar to earlier studies (Dong et al., 2005, 2006). Briefly, once a day for 5 d, rats (~32 d old) were taken out of the home cage for an intraperitoneal injection of either (−)cocaine HCl (15 mg/kg in saline) or the same volume of saline, and placed back to the home cage immediately. Thus, the contextual cues associated with cocaine injection (Badiani et al., 1997) was not intentionally provided. Cocaine/saline-treated rats were then used for electrophysiological recordings either ~48 h or 21 d following the last injection.

Virus preparation and in vivo *delivery.* The lentiviral vectors expressing GFP, PSD95-GFP, and PSD95-RNAi-GFP were made as described previously (Schlüter et al., 2006). Briefly, the lentiviral vector constructs were modified from the original FUGW vector backbone (Lois et al., 2002). For shRNA expression, an H1 promoter cassette from pSuper vector, including a hairpin (sh95) targeting the PSD-95 sequence GGA CAT CCA GGC ACA CAA G, was cloned between the HIV-flap and ubiquitin promoter. The eGFP was driven by the ubiquitin promoter. For production of viral vectors, the transfer vector, the HIV-1 packaging vector Δ8.9, and the VSVG envelope glycoprotein vector were cotransfected into HEK293 fibroblasts using FUGENE6 transfection reagent (Roche). Supernatants of culture media were collected 48 h after transfection and centrifuged at 50,000 × g to concentrate the viral vector. The titer of the virus was estimated by detecting the infection rate of the virus in the dissociated hippocampal neuronal cultures. Typically, 1 μl of the concentrated viral solution was dropped into a 10 cm culture dish (containing ~6000 cell/cm^2 primary hippocampal neurons in N-2 supplemented MEM plus GlutaMax, Invitrogen). Seven days later, the infection rate (GFP-positive cells/total cells) was measured. Only the viral solutions with >80% infection rates (high titers) were used for experiments involving *in vivo* viral infection.

To infect the *in vivo* NAc shell MSNs, a stereotaxic microinjection technique was used. Briefly, rats were anesthetized with pentobarbital and a stainless-steel cannula was implanted bilaterally into the NAc shell (in mm: A, 1.5; L, 0.6; D, 6.5). Concentrated viral solutions (1 μl/side) were infused into the NAc shell through a pump at a flow rate of 0.2 μl/min. The injection cannula was then slowly withdrawn and the rats were then placed on the warmed heating pad for postsurgical recovery. After waking up, rats were then transferred to regular housing cages.

The electrophysiological experiments using virally infected MSNs were performed ~7–10 d following the viral injection. Infected neurons were identified in living slices by their GFP signals using epifluorescence microscopy. Typically, >20 PFG-positive MSNs could be identified as healthy neurons in each slice, and these infected MSNs were mostly clustered within a ~5 mm radius of the injection spot. We normally selected the infected MSN with similar morphological properties as their neighbor uninfected MSNs (uninf). In addition, we also measured the basic electrophysiological properties of the intended infected MSNs. For example, when measured with Cs^+-based internal solution (for recording synaptic current), NAc MSNs infected by these viruses exhibited similar break-in resting membrane potential (in mV: uninf, −70.4 ± 1.6, $n = 22$; GFP, −68.1 ± 2.4, $n = 7$) and membrane resistance (in MΩ: uninf, 146.5 ± 5.7, $n = 22$; GFP, 138.4 ± 6.3, $n = 7$) as observed in uninfected MSNs, suggesting that the lentivirus-associated toxicity was minimal.

NAc slice culture, cell selection, and electrophysiology. Detailed procedure for obtaining and culturing NAc slices can be found in our previous publications (Dong et al., 2006; Huang et al., 2008; Lee et al., 2008). Briefly, for slice cultures, younger rats (~19 d old) were used. They were deeply anesthetized with isoflurane and decapitated. Coronal NAc slices (200 μm thick) were obtained (normally two to three slices were obtained from each rat) in ice-cold sterile low-Ca^{2+} solution containing the following (in mM): 126 NaCl, 1.6 KCl, 1.2 NaH_2PO_4, 1.2 $MgCl_2$, 0.625 $CaCl_2$, 18 $NaHCO_3$, and 11 glucose, and then placed on Millicell Millipore culture plate inserts in wells containing Neurobasal-A media with 4% B-27 and 1% GlutaMax-I supplements (Invitrogen) for ~24 h until it is transferred to the recording media for electrophysiological recordings. For acute NAc slice, 32- to 40-d-old rats (2 d withdrawal) or ~57-d-old rats were used. Coronal slices of 250–300 μm thickness were then cut such that the preparation contained the signature anatomical landmarks (e.g., the anterior commissure) that delineated the NAc subregions. Acute slices were submerged in a recording chamber and were continuously perfused with regular oxygenated aCSF (in mM: 126 NaCl, 1.6 KCl, 1.2 NaH_2PO_4, 1.2 $MgCl_2$, 2.5 $CaCl_2$, 18 $NaHCO_3$, and 11 glucose, 295–305 mOsm, equilibrated at 31–34°C with 95% O_2/5% CO_2).

Electrophysiological recordings were preferentially made from the MSNs located in the ventral–medial subregion of the NAc shell, which could be identified by anatomical landmarks, such as the anterior commissure. MSNs in this subregion have been shown to be importantly implicated in a variety of addiction-related molecular, cellular, and behavioral alterations (Kelley, 2004; Dong et al., 2006; Huang et al., 2008). The MSNs, which comprise >90% of all neuronal types in the NAc, could be readily identified in the experimental condition by their mid-sized somas as well as their electrophysiological characteristics, such as hyperpolarized resting membrane potentials, long latency before the first action potential, lack of the I_h component, and rectification of the *I–V* curve at hyperpolarized voltages (Wilson and Groves, 1980; Dong et al., 2006).

Standard whole-cell recordings were made using a MultiClamp 700B amplifier (Molecular Devices) through an electrode (2–6 MΩ) in all electrophysiological experiments (Saal et al., 2003; Dong et al., 2004, 2006; Huang et al., 2008). Current-clamp recordings were used to measure evoked action potential firing, in which the resting membrane potential was normalized to −80 mV in acute slice and −70 mV in slice cultures. For these experiments, a K^+-based internal solution was used (in mM: 130 K-methanesulfate, 10 KCl, 10 HEPES, 0.4 EGTA, 2.0 $MgCl_2$, 2.5 MgATP, 0.25 Na_3GTP, pH 7.2–7.4; 275–285 mOsm). Voltage-clamp recordings were used to measure EPSCs, in which AMPAR EPSCs were measured at the holding potential of −70 mV in the presence of 100 μM picrotoxin; NMDAR EPSCs were measured at either +50 mV or −40 mV in the presence of 100 μM picrotoxin and 10 μM 2,3-dihydroxy-6-nitro-7-sulfamoyl-benzo[*f*]quinoxaline-2,3-dione (NBQX). For these experiments, a Cs^+-based internal solution was used (in mM: 117 cesium methanesulfonic acid, 20 HEPES, 0.4 EGTA, 2.8 NaCl, 5 TEA-Cl, 2.5 MgATP, 0.25 Na_3GTP, pH 7.2–7.4; 275–285 mOsm). Picrotoxin (100 μM), which blocked $GABA_A$R-mediated currents, was only used in experiments isolating EPSCs and EPSPs (see Figs. 2*A–D*, 4*A–D*, 6*A*; supplemental Fig. S1, available at www.jneurosci.org as supplemental material), but not in those involving pharmacological incubation of slices and measurement of action potential firing. When measuring EPSCs, presynaptic stimuli (intensity, 40–65 μA; duration, 65–95 μs; frequency, 0.1 Hz; ~100 μm to recorded neurons) were applied through a monopolar microelectrode. Amplitudes of AMPAR EPSCs were calculated by averaging ~25 EPSCs at −70 mV and measuring the peak (2 ms window) compared with the baseline (2 ms window). NMDAR EPSC amplitudes were calculated by averaging ~13 EPSCs and measuring the amplitude (2 ms window) either at 40 ms after the EPSC onset (when recorded at +50 mV) or the peak (when recorded at −40 mV).

Pairwise recordings (Marie et al., 2005) were used to compare AMPAR and NMDAR EPSCs between virally infected and uninfected NAc MSNs. Briefly, an infected and an uninfected MSN that were anatomically adjacent to each other were identified as a cell pair. One of these cells was recorded first and the stimulator position, intensity, and frequency were set to evoke stable EPSCs. After measuring EPSCs at both −70 mV and +50 mV, recordings were quickly made from the other cell without altering any of the preset stimulus parameters. As previously described and verified (Marie et al., 2005), the amplitude of AMPAR EPSCs were measured at the peak at −70 mV and the amplitude of NMDAR EPSCs were measured at 50 ms after EPSC onset at +50 mV. The measurement of NMDAR EPSC amplitude was further confirmed using the selective AMPAR antagonist NBQX (data not shown). The amplitudes of AMPAR and NMDAR EPSCs in infected cells were directly compared with those in uninfected cells and the relative values were obtained. The afterhyper-

polarization potential (AHP) was sampled following the first action potential spike, usually elicited by the rheobase stimulation.

D-APV (referred to as APV throughout the manuscript), NBQX, bafilomycin A1, apamin and iberiotoxin (IbTx) were purchased from Tocris. D-Cycloserine (DCS) was purchased from RPI, and other chemicals were purchased from Sigma-Aldrich.

Data acquisition, analysis, and statistics. Normally, one or two cells were obtained from one rat. Numbers of examined cells (n) and animals (m) are presented as "n/m" in the manuscript. "n" was used in all statistics. In experiments involving viral-mediated manipulations, data were blindly obtained; the experimenters were not aware of the types of viruses injected until the late stage of data analysis. All results are shown as mean ± SEM. Two-factor repeated-measures ANOVA was used in most analyses (see Figs. 1–3, 4*E–H*, 5, 6, 8; supplemental Fig. S2, available at www.jneurosci.org as supplemental material). In these analyses, factor A was assigned for the treatments (with multiple levels: pharmacological treatments in Figs. 1, 2, 5*D*,*F*, 7*K*,*L*, and 8*A*, or time points in Figs. 3 and 5*A*,*B*). Factor B was assigned for current injections (2 levels, 100 and 200 pA, in Figs. 1 and 2; 9 levels, 0–400 pA with a 50 pA interval in Figs. 3–8). The related statistical results were primarily presented in the F and p values of the main effect of factor A, which was our primary research interest (the effect of pharmacological treatments/time on membrane excitability). Degrees of freedom of between (b) and within treatments (w) were presented as $F_{(b,w)}$. For results with factor A containing >2 levels, a Bonferroni posttest was performed when significance was obtained. To estimate the effect size (see Figs. 3*B*, 5*B*), the mean number of action potentials at each level in factor A was used to perform a cross-level comparison. Independent (see Fig. 7*A–E*,*H–J*,*N*) or paired t test (supplemental Fig. S2, available at www.jneurosci.org as supplemental material) was used for the rest of the data analysis except in Figure 4, *B* and *D*, and Figure 8, *B* and *C*, in which one-factor repeated-measures ANOVA was used, followed by Bonferroni posttests. The F and p values were presented in the Results section; the related descriptive values (e.g., means. SE) and the results from posttests were presented in the supplemental material (available at www.jneurosci.org).

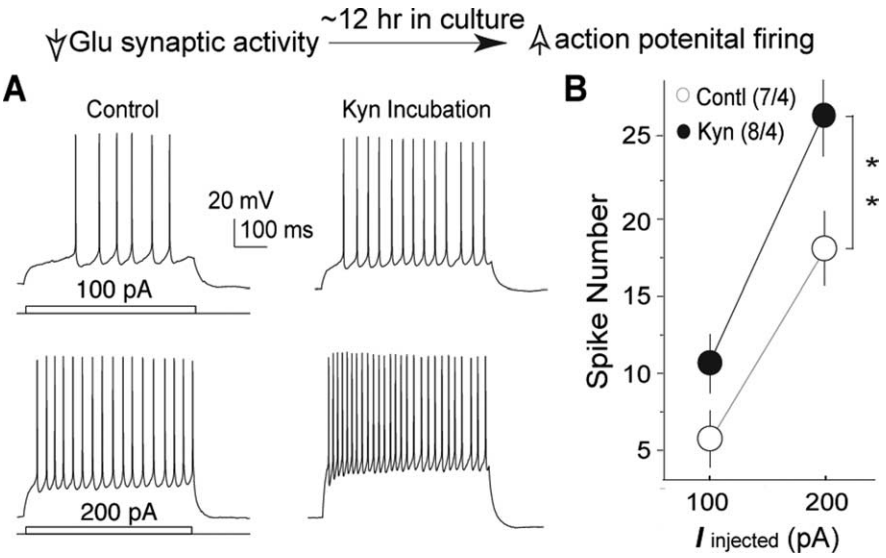

Figure 1. *h*SMP in NAc MSNs in slice cultures. ***A***, Example action potential firings evoked by 100 and 200 pA (500 ms) in NAc MSNs in slice cultures without pharmacological treatment (left) and with 12 h incubation of 2 mM glutamate receptor antagonist Kyn (right). ***B***, A summary showing that the evoked action potential firing was homeostatically increased in NAc MSNs upon a persistent decrease in the excitatory synaptic activity. $^{**}p < 0.01$; (n/m), number of cells/number of animals.

Results

*h*SMP in NAc slice cultures

In 1-d-old slice cultures, NAc neurons exhibited stable intrinsic membrane excitability (Dong et al., 2006) and spontaneous excitatory synaptic inputs that are much more extensive than in acutely prepared slices (Huang et al., 2008; Lee et al., 2008). The frequency of evoked action potentials is often used to detect the intrinsic membrane excitability (Desai et al., 1999; Nelson et al., 2003; Zhang and Linden, 2003). To detect potential *h*SMP, we used a whole-cell current-clamp technique to examine the evoked action potential firing (by current steps of 100 and 200 pA, 500 ms; membrane potential was adjusted at −70 mV) of NAc neurons with synaptic manipulations. Following chronic (~12 h) incubation of kynurenic acid (Kyn, 2 mM), which inhibited the basal excitatory synaptic activities (nonpharmacological treatment as control), the number of evoked action potentials in NAc neurons was significantly increased ($F_{(1,26)} = 13.1$, $p < 0.01$) (Fig. 1). These results suggest that NAc MSNs can adjust the membrane excitability (output) to functionally compensate for the alteration in synaptic input (input intensity) such that the integration of input-to-output may remain stable. This synapse-to-membrane modulation is referred to as "homeostatic synapse-driven membrane plasticity (*h*SMP)."

NMDARs mediate *h*SMP

Synaptic NMDARs act as both detectors of synaptic activity (Malenka and Nicoll, 1999) and regulators of intrinsic membrane excitability (Zhang and Linden, 2003; Xu et al., 2005). In NAc slice cultures, synaptic NMDARs are tonically active and are critical for the synapse–membrane interaction (down state–up state oscillation) (Huang et al., 2008). The next question was whether manipulating NMDARs alone was sufficient to induce *h*SMP. We first verified that two pharmacological agents could chronically increase or decrease the basal NMDAR activity in NAc slice cultures. Using whole-cell voltage-clamp technique ($V_H = -40$ mV, in the presence of the $GABA_A$ and AMPA receptor antagonists picrotoxin at 0.1 mM and NBQX at 10 μM), we recorded NMDAR-mediated excitatory postsynaptic currents (EPSCs) from NAc neurons (Fig. 2). Application of D-cycloserine (DCS, 10 μM), an NMDAR coagonist, enhanced the peak amplitude of NMDAR EPSCs by 47% (± 4%, n/m = 7/4) (Fig. 2*A*,*B*). Furthermore, NMDAR EPSCs measured in DCS could be completely blocked by NMDAR antagonist APV (50 μM), indicating that the DCS-enhanced portion of EPSCs was mediated by NMDARs. We then verified that APV at 5 μM could inhibit the peak amplitude of NMDAR EPSCs by 71% (± 6%, n/m = 9/5) (Fig. 2*C*,*D*). Thus, applications of 10 μM DCS and 5 μM APV could increase and decrease the NMDAR activity, respectively. We then incubated the NAc slice cultures with either DCS or APV and ~12 h later measured the evoked action potential firing. We observed that incubation with DCS significantly decreased action potential firing in NAc neurons, whereas incubation with APV induced the opposite effect ($F_{(2,48)} = 12.8$, $p < 0.01$) (Fig. 2*E*,*F*).

To clarify whether the effect of NMDARs was a gradually occurring homeostatic response or simply an acute receptor-mediated regulation of membrane excitability, we examined the evoked action potential firing of NAc neurons in response to acute manipulations of NMDAR activity. Upon acute applications (perfusion for ~15 min) of either DCS ($F_{(1,20)} = 0.03$, p =

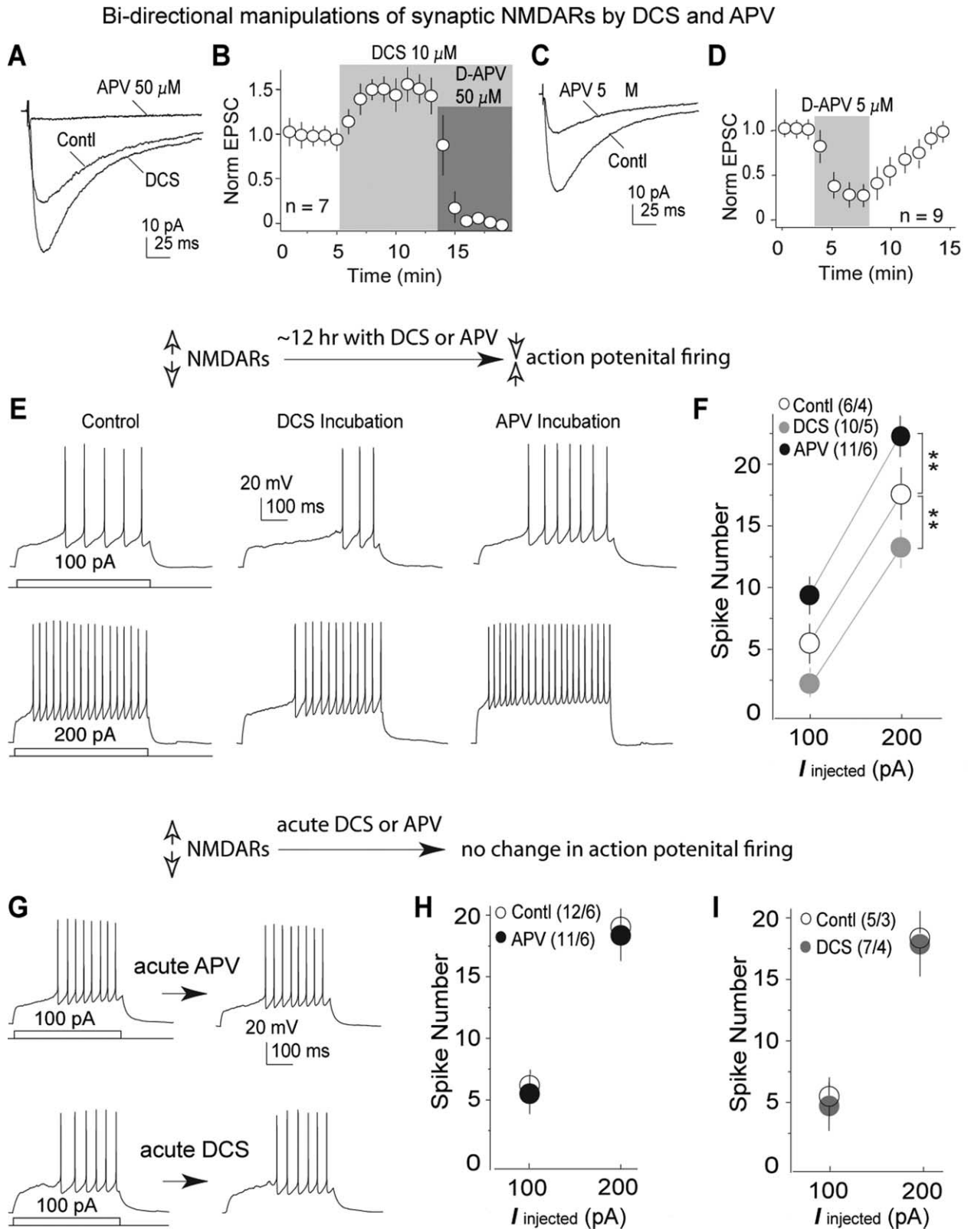

Figure 2. NMDARs mediate *h*SMP in slice cultures. ***A***, An example NAc MSN in which the NMDAR EPSC (recorded at −40 mV) was enhanced by application of NMDAR coagonist DCS (10 μM) and the NMDAR EPSC in the presence of DCS was completely inhibited by the NMDAR antagonist APV (50 μM). ***B***, A summary showing that application of DCS increased the amplitude of NMDAR EPSCs in NAc MSNs by ~47%, and that NMDAR EPSCs in DCS were completely inhibited by application of APV. ***C***, An example NAc MSN in which the NMDAR EPSC was partially inhibited by a low concentration (5 μM) of APV. ***D***, A summary showing that application of 5 μM APV inhibited NMDAR EPSCs in NAc MSNs by ~71%. ***E***, Action potential firings (evoked by 100 and 200 pA, 500 ms) in three example NAc MSNs in slice cultures without pharmacological treatment (control, left), and treated with 10 μM DCS (middle) or 5 μM APV (right). ***F***, A summary showing that in NAc MSNs, a persistent increase or decrease in the NMDAR activity induced a decrease or increase in the evoked action potential firing, respectively. ***G***, Action potential firings (evoked by 100 pA, 500 ms) from two example NAc MSNs with acute perfusion of 5 μM APV (upper) or 10 μM DCS (lower). ***H***, ***I***, Summaries showing that an acute decrease (by APV) or increase (DCS) in NMDAR activity did not affect the action potential firing in NAc MSNs in slice cultures. $^{**}p < 0.01$; (*n*/*m*), number of cells/number of animals.

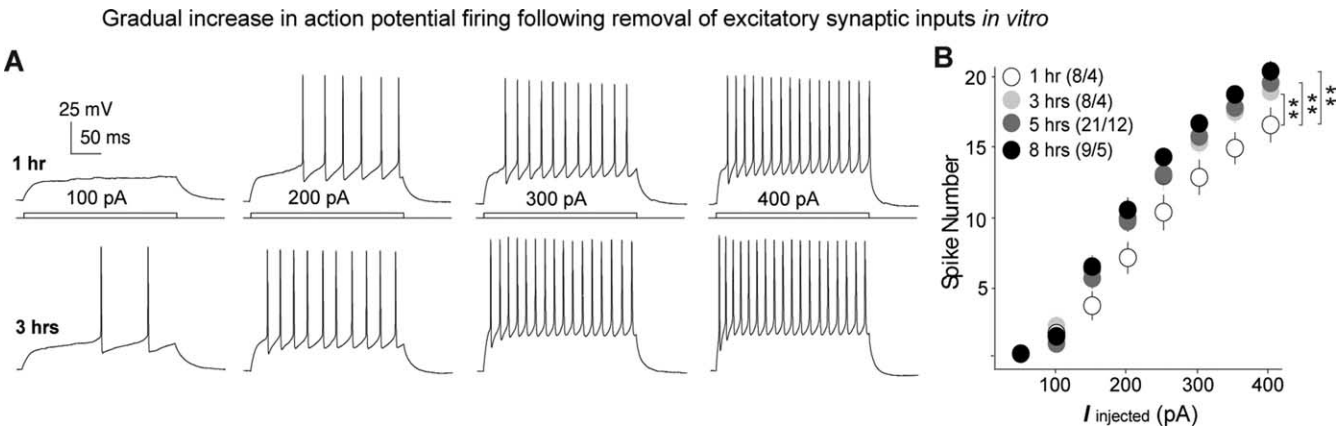

Figure 3. Homeostatic increase in action potential firing of NAc MSNs after removal of most synaptic inputs. ***A***, Action potential firings (evoked by 100, 200, 300, and 400 pA, 300 ms) from two example NAc MSNs in acute slices maintained 1 (upper) or 3 h (lower) after slice preparation. ***B***, A summary showing that the action potential firing of NAc MSNs in acute slices was gradually and progressively increased after slice preparation. $^{**}p < 0.01$; (*n*/*m*), number of cells/number of animals.

0.86) (Fig. 2*G*,*I*) or APV ($F_{(1,42)} = 0.22$, $p = 0.91$) (Fig. 2*G*,*H*), the numbers of evoked action potentials were not significantly altered. Collectively, our results suggest that *h*SMP in NAc MSNs is a gradually occurring process in which NMDARs play a key role.

*h*SMP in acute brain slices

The *in vivo* NAc MSNs are extensively innervated and tonically activated by excitatory synaptic inputs (O'Donnell and Grace, 1995). Such high basal activity of excitatory synapses is usually not present in acutely prepared brain slices (Lee et al., 2008). Thus, if *h*SMP functions well, it would be expected that the membrane excitability of NAc MSNs is homeostatically and gradually upregulated after preparation of acute slices. Consistent with this prediction, the number of evoked action potentials in NAc MSNs gradually increased with time after brain slice preparation (measured at 1 h, 3 h, 5 h, and 8 h following the preparation of acute slices; current steps: amplitude, 50–400 pA, with a 50 pA increment; duration, 300 ms; membrane potential was normalized to −80 mV) ($F_{(3,249)} = 14.8$, $p < 0.01$; the effect size of time was estimated by the "mean difference" between 1 h and other time points: 3 h, 1.90; 5 h, 1.92; 8 h, 2.73) (Fig. 3). Thus, potentially through *h*SMP, the membrane excitability of NAc MSNs homeostatically and gradually increased in acute brain slices.

We next examined whether *h*SMP is fully functional in acute slices. If so, we expect the membrane excitability of NAc MSNs to be homeostatically regulated upon alterations in excitatory synaptic activities. Unlike in slice cultures, the NAc MSNs in acute slices do not normally exhibit membrane potential oscillations and mostly dwell at very negative membrane potentials (Wilson and Kawaguchi, 1996; Huang et al., 2008; Lee et al., 2008). Because of this, we examined whether the basal excitatory synaptic inputs to NAc neurons in acute slices can be experimentally manipulated with the pharmacological tools established in slice cultures (Fig. 2). We recorded spontaneous EPSPs (sEPSPs, in the presence of 0.1 mM picrotoxin) in the resting NAc neurons within acute brain slices (at resting membrane potential) (Fig. 4*A*). By detecting their sharp rising peak, individual sEPSP events were able to be distinguished (indicated by arrows in Fig. 4*A*), and thus were used to measure the frequency of sEPSPs. We observed that application of either DCS or DCS together with APV did not affect the frequency of sEPSPs ($F_{(2,12)} = 0.78$, $p = 0.49$) (Fig. 4*B*), suggesting that the basal presynaptic release of glutamate was not substantially affected by these two pharmacological manipulations. On the other hand, sEPSPs were heavily overlapped (Fig. 4*A*) such that the amplitude of individual sEPSP could not be precisely measured. Instead, we determined the effect of DCS (10 μM) or APV (50 μM) on sEPSP amplitude by measuring the integrated area, defined as the net change of the membrane potential (active membrane potential − baseline) multiplied by the recording duration (11 s, sum of 10 consecutive traces) (Fig. 4*C*). The integrated area was significantly increased by application of DCS, and an additional application of APV decreased the integrated area to the baseline level ($F_{(2,15)} = 6.27$, $p < 0.01$) (Fig. 4*D*). These results suggest the following in acute NAc slices: (1) Application of DCS potentiated the NMDAR-mediated synaptic component even at the resting membrane potential at which the Mg^{2+}-mediated blockade of NMDARs is significant (but not complete) (Jahr and Stevens, 1990). Thus, the application of DCS remained as an effective pharmacological tool in acute slices. (2) The application of APV did not significantly inhibit NMDAR-mediated synaptic transmission of NAc neurons in the acute slice, which may be due to the already low activity of NMDARs at hyperpolarized resting membrane potentials (Fig. 4*D*). Thus, in acute slices, application of APV may not be an effective approach to trigger *h*SMP, and in the following experiments involving acute NAc slices we therefore primarily focused on one direction of *h*SMP, the increase in NMDAR sEPSPs leading to a decrease in membrane excitability.

After incubating the acute slices with DCS (10 μM) for >5 h, we measured the action potential firing of NAc MSNs. Due to the continual upward drift of membrane excitability of NAc MSNs over the *in vitro* time (Fig. 3), we defined the baseline control as the membrane excitability measured at the same *in vitro* time point but without any pharmacological treatment. Compared with controls, NAc MSNs with DCS incubation exhibited a significantly lower level of membrane excitability ($F_{(1,105)} = 5.83$, $p < 0.05$) (Fig. 4*E*,*F*), and the effect of DCS was more pronounced upon higher injected currents ($F_{(1,105)} = 4.49$, treatment × current injection; $p < 0.05$ at 250–400 pA, posttest). In addition, a 5 h incubation of D-serine (10 μM), the endogenous coagonist for NMDARs, also decreased the number of evoked action potential firings in NAc MSNs ($F_{(1,119)} = 6.77$, $p < 0.05$) (Fig. 4*G*,*H*). Similarly, the effect of D-serine was more pronounced upon higher injected currents ($F_{(1,119)} = 5.66$, treatment × current injection; $p < 0.05$ at 200–400 pA, posttest).

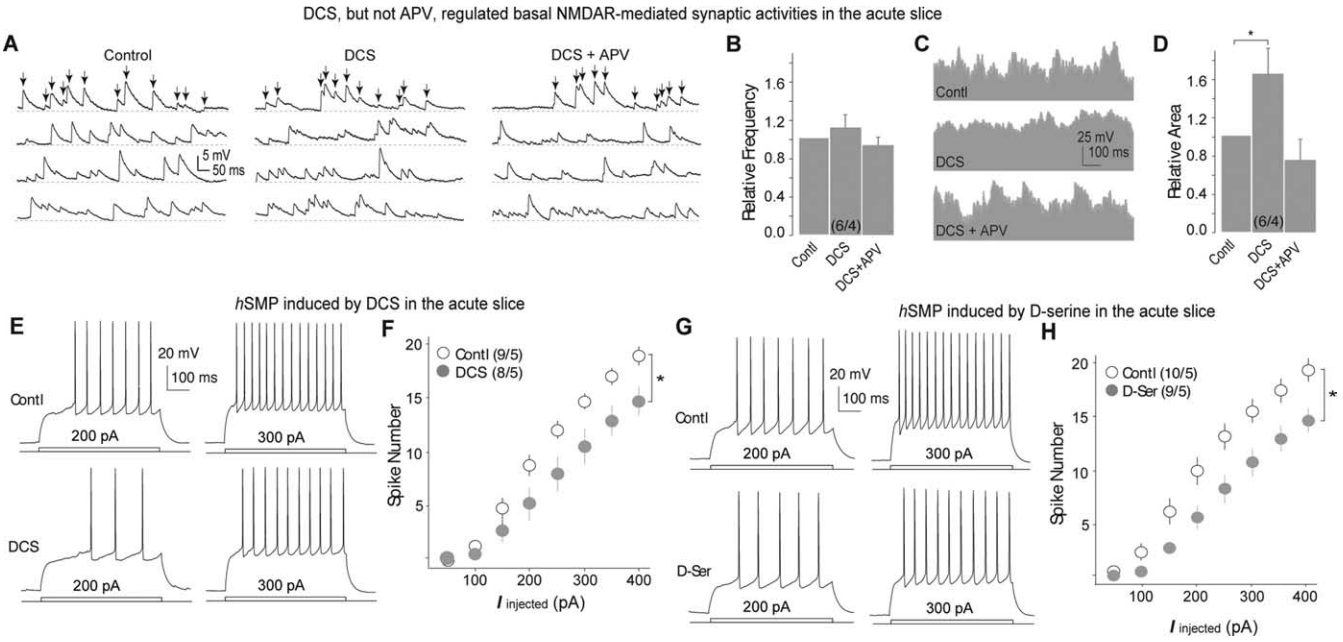

Figure 4. *h*SMP in acute brain slices. ***A***, Spontaneous EPSPs in an example NAc MSN (recorded at the resting membrane potential, −78 mV) before pharmacological treatment (left) and during the treatment of DCS (middle) or DCS + APV (right). ***B***, A summary showing that the frequency of sEPSPs was not affected by application of DCS or DCS + APV. Events were visually identified as indicated by the arrows in ***A***. ***C***, Integrated areas of sEPSPs of the same neuron in ***A*** in the treatments of control, DCS, and DCS + APV. ***D***, A summary showing that the integrated area of sEPSPs of NAc MSNs was increased by incubation of DSC, and that this increase was abolished by APV. ***E***, Action potential firings (elicited by 200 and 300 pA, 300 ms) from two example NAc MSNs incubated with control aCSF (upper) or DCS (lower) for 5 h. ***F***, A summary showing that persistent potentiation of the NMDAR activity by DCS homeostatically decreased the evoked action potential firing in NAc MSNs. ***G***, Action potential firings (elicited by 200 and 300 pA, 300 ms) from two example NAc MSNs incubated with control aCSF (upper) or D-serine (lower) for 5 h. ***H***, A summary showing that incubation of D-serine homeostatically decreased the action potential firing in NAc MSNs. *$p < 0.05$; (*n*/*m*), number of cells/number of animals.

Together, these results suggest that *h*SMP is an endogenous homeostatic mechanism that can be detected in both NAc slice cultures and acutely prepared NAc slices.

We next determined the time course of *h*SMP-mediated downregulation of membrane excitability in acute slices. We measured the evoked action potential firing at 10 min, 3 h and 5 h during the incubation with 10 μM DCS (slices with the same μtime but without pharmacological treatment were used as controls) and observed that the membrane excitability was gradually decreased over this time course ($F_{(1,70)} = 0.18$, $p = 0.99$, 10-min DCS vs control; $F_{(1,105)} = 2.1$, $p = 0.047$, 3 h DCS vs control; $F_{(1,259)} = 10.77$, $p < 0.01$, 5 h DCS vs control) (Fig. 5*A*). Furthermore, when the DCS-treated brain slices (5 h) were washed in a DCS-free bath for 3 h, the NAc MSNs still exhibited a significantly lower rate of action potential firing than MSNs without treatment for 8 h ($F_{(1,91)} = 12.94$, $p < 0.01$, 5 h DCS + 3 h wash vs control) (Fig. 5*A*). This set of results (summarized in Fig. 5*B*) indicated that *h*SMP developed gradually and was reversed slowly.

Presumably due to the low level of NMDAR activity at hyperpolarized resting membrane potentials in acute slices, application of APV did not significantly decrease the basal NMDAR-mediated synaptic transmission (Fig. 4). Thus, it was predicted that incubation with APV should not induce *h*SMP in NAc neurons in the acute slice. As predicted, incubation with APV at two concentrations (5 and 50 μM, 5 h) did not affect the evoked action potential firing ($F_{(2,119)} = 0.11$, $p = 0.90$) (Fig. 5*C*,*D*). Although application of APV did not further inhibit the basal NMDAR-mediated activity, it prevented DCS-induced potentiation of NMDAR sEPSPs (Fig. 4*B*,*C*). Consequently, we observed that coincubation with 50 μM APV prevented DCS-induced *h*SMP in NAc MSNs in acute slices, whereas coincubation with a low concentration (5 μM) of APV, which partially inhibited NMDAR-mediated synaptic transmission (Fig. 2*D*), partially inhibited DCS-induced *h*SMP ($F_{(3,255)} = 19.85$, $p < 0.01$; posttest, $p = 1.0$, control vs DCS + 50 μM APV) (Fig. 5*E*,*F*).

Synapse-specific *h*SMP

The pharmacological manipulations used above affected both synaptic and nonsynaptic NMDARs, raising a concern that nonsynaptically located NMDARs may be implicated in the observed *h*SMP. In an attempt to focus on the synaptic activity in *h*SMP, we adopted two independent approaches. One approach involved using a plecomacrolide antibiotic, bafilomycin A1 (Baf), which inhibits H^+-ATPase-dependent reassembly of presynaptic vesicles, and has been used as a pharmacological tool to deplete synaptic transmission (Zhou et al., 2000; Cavelier and Attwell, 2007; Ziskin et al., 2007). Thus, if *h*SMP is driven by excitatory synapses, it should not be induced following Baf-mediated depletion of synaptic transmission. The efficiency of Baf was verified first by incubating the NAc slices with 1 μM Baf for 1–6 h. We observed that the frequency of sEPSPs in NAc neurons was substantially decreased along the course of Baf incubation (in Hz: 0 h, 6.4 ± 1.7, *n*/*m* = 5/3; 1 h, 1.30 ± 0.42, *n*/*m* = 4/3; 2 h, 0.45 ± 0.05, *n*/*m* = 7/4; 6 h, 0.05 ± 0.01, *n*/*m* = 11/6; non-Baf treatment control at 6 h, 6.1 ± 0.9, $n = 4$) (Fig. 6*A*), indicating that the Baf incubation could effectively deplete the synaptic transmission to NAc neurons in acute slices. We next demonstrated that incubation with Baf for 6 h alone did not changed the evoked action potential firing in NAc MSNs ($F_{(1,126)} = 0.05$, $p = 0.82$) (Fig. 6*B*). After this verification, we preincubated the NAc slices with Baf for 2 h and then incubated the slices with DCS for ~4 h (in the presence of Baf). We observed that DCS-induced *h*SMP was abolished by the Baf incubation ($F_{(2,192)} = 21.4$, $p < 0.01$) (Fig. 6*C*).

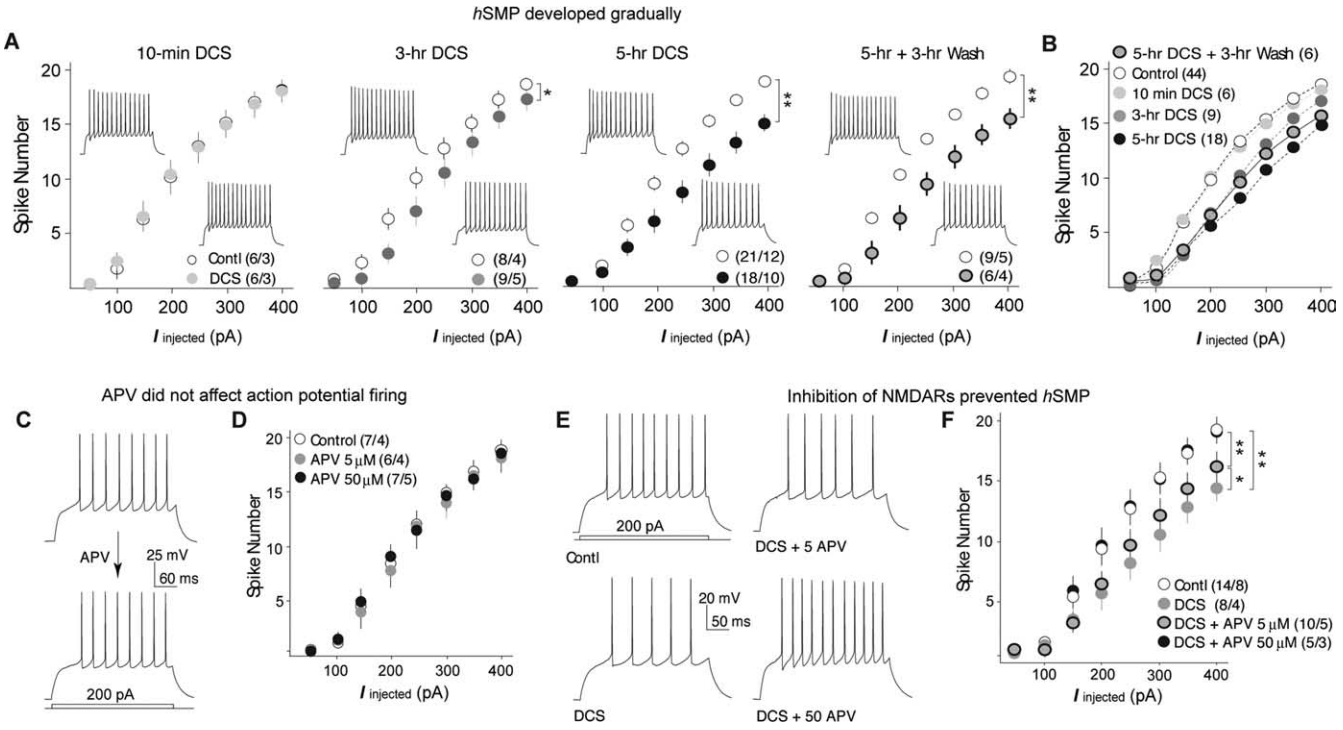

Figure 5. Time- and dose dependence of *h*SMP in acute slices. ***A***, Summaries showing that the action potential firing of NAc MSNs decreased gradually along the course of DCS incubation and the DCS-induced decrease in action potential firing remained up to 3 h after DCS was washed. Insets showing the action potential firings elicited by 300 pA, 300 ms current pulses in control (upper) and DCS-treated (lower) NAc MSNs in each condition. ***B***, A summary of the data presented in ***A***. ***C***, Action potential firings (elicited by 200 pA, 300 ms) from an example NAc MSN before (upper) and after (lower) incubation of 50 μM APV. ***D***, A summary showing that incubation of APV (5 or 50 μM) did not affect the action potential firing in NAc MSNs. ***E***, Action potential firings from four example NAc MSNs in acute slices treated with 5 h incubation of control aCSF, 10 μM DCS, 10 μM DCS + 5 μM APV, and 10 μM DCS + 50 μM APV. ***F***, A summary showing that DCS-induced *h*SMP was dose-dependently inhibited by APV. $^*p < 0.05$; $^{**}p < 0.01$; (*n*/*m*), number of cells/number of animals.

Thus, *h*SMP cannot be induced in the absence of presynaptic releases.

In another approach, we took advantage of the *in vivo* property of NAc MSNs, which normally received relatively constant tonic synaptic AMPAR and NMDAR activities. Thus, a chronic shift of the excitatory synaptic strength may trigger *h*SMP in the *in vivo* NAc MSNs. Because the *h*SMP-mediated changes in membrane excitability reversed slowly (Fig. 5*A*), the *in vivo h*SMP should be detectable immediately after slice preparation. To experimentally increase or decrease the excitatory synaptic strength (mainly mediated by synaptic AMPARs and detected by NMDARs) in NAc MSNs *in vivo*, we developed a lentiviral system-based approach and validated that in *in vivo* NAc MSNs, expression of PSD95 or the interference RNA (RNAi) of PSD95 increased or decreased the excitatory synaptic strength, respectively (supplemental material, available at www.jneurosci.org). Hence, we used these *in vivo* manipulations in a set of double-blind experiments (see Materials and Methods) to determine the role of excitatory synapses in *h*SMP *in vivo*. Briefly, 7–11 d after the intra-NAc injections of viruses expressing GFP (control), PSD95-GFP, or PSD95-RNAi-GFP, the NAc slices were obtained and recordings immediately taken. Comparison of the virally infected MSNs with their uninfected (uninf) neighbor cells revealed that PSD95-RNAi-expressing NAc MSNs exhibited an increase, whereas the PSD95-expressing neurons exhibited a decrease, in the evoked action potential firing ($F_{(3,320)} = 28.3$, $p < 0.01$) (Fig. 6*F*,*G*). Together, the above results suggest that the identified *h*SMP is initiated by synaptically located substrates.

SK channels mediate the expression of *h*SMP

In an attempt to determine the key ionic conductances through which *h*SMP was expressed, we compared both the positive and negative membrane properties between NAc MSNs with and without DCS-induced *h*SMP. Consequently, we singled out the afterhyperpolarization potential (AHP), which normally functions to suppress the generation of subsequent action potentials (for other electrophysiological parameters, see supplemental material, available at www.jneurosci.org). To quantify the changes in different components of AHP, the peak of AHP (~3 ms after the onset of action potential) was operationally defined as the fast component of AHP (*f*AHP), and the membrane potential at 10 ms after the onset of action potential was defined as the medium component (*m*AHP) (Fig. 7*A*). The *m*AHP ($t_{(37)} = -2.78$, $p < 0.01$), but not *f*AHP ($t_{(37)} = -1.17$, $p = 0.25$), was significantly increased in NAc MSNs expressing *h*SMP (traces shown were the averaged traces of all recorded neurons in each group) (Fig. 7*A–C*).

Two ionic candidates mediating AHP were the BK and SK types Ca^{2+}-activated K^+ channels, both of which are present in NAc MSNs (Chang et al., 1997; Sailer et al., 2002). We first examined the potential involvement of BK channels. Acute application of the BK channel-selective antagonist iberiotoxin (IbTx, at 100 nM) significantly decreased *f*AHP without affecting *m*AHP in NAc MSNs in control slices (*f*AHP, $t_{(4)} = 3.53$, $p < 0.05$; *m*AHP, $t_{(4)} = 1.08$, $p = 0.34$) (Fig. 7*D–F*), indicating that the defined *f*AHP in NAc MSNs was primarily mediated by BK channels. Blockade of BK channels by acute application of 100 nM

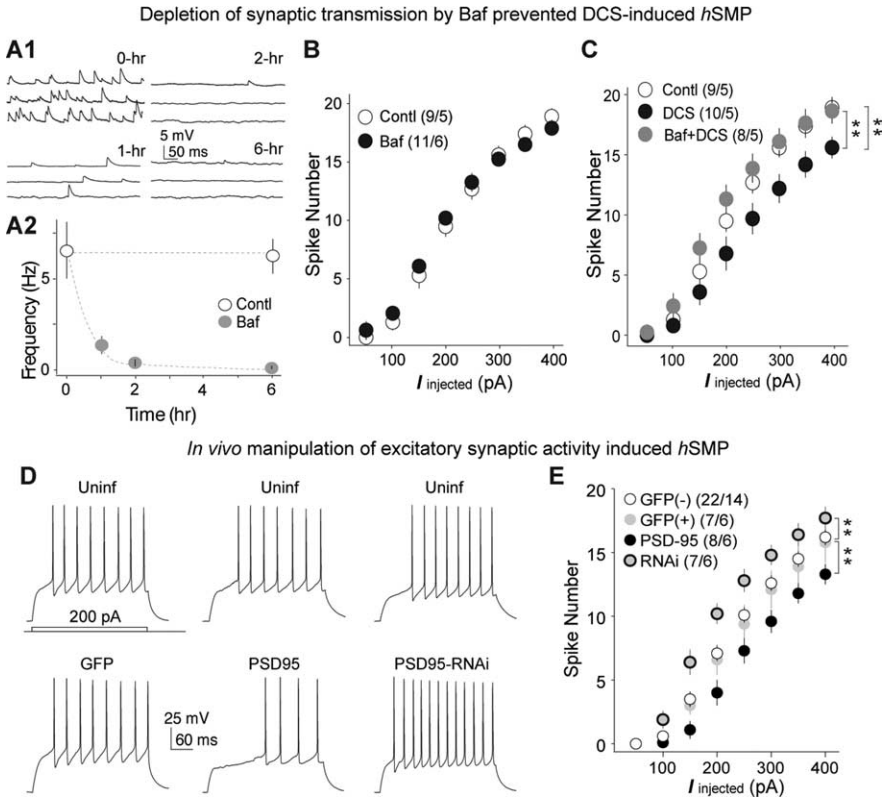

Figure 6. Synapse-specificity of *h*SMP. ***A1***, Spontaneous EPSPs from four example NAc MSNs with 0, 1, 2, or 6 h incubation of 1 μM Bafilomycin (Baf). ***A2***, A summary showing that the frequency of sEPSPs in NAc MSNs was progressively decreased by Baf over incubation time. ***B***, A summary showing that 6 h incubation with Baf alone did not alter the action potential firing in NAc MSNs in acute slices. ***C***, A summary showing that incubation of Baf abolished DCS-induced *h*SMP in NAc MSNs in acute slices. ***D***, Action potential firings (elicited by 200 pA, 300 ms) from example pairs, uninfected MSNs versus PSD95-manipulated MSNs. ***E***, A summary showing that an increase in excitatory synaptic strength by overexpressing PSD95 decreased the intrinsic membrane excitability of NAc MSNs, whereas a decrease in excitatory synaptic strength by expressing PSD95-RNAi caused the opposite effect. $^{**}p < 0.01$; (*n*/*m*), number of cells/number of animals.

IbTx to acute slices (without DCS treatment) did not significantly alter the evoked action potential firing in NAc MSNs ($F_{(1,56)} = 0.99$, $p = 0.35$) (Fig. 7*G*). These results suggest that due to the compounded effect of BK channels on membrane excitability (see Discussion), BK channels and the *f*AHP may not sensitively regulate the action potential firing in NAc MSNs, and thus were not likely to be the expression site for *h*SMP.

We next examined the involvement of SK channels in *h*SMP by using the SK channel-selective antagonist apamin. In NAc neurons without DCS incubation, application of apamin (300 nM) did not affect either *f*/*m*AHP (*f*AHP, $t_{(4)} = 1.43$, $p = 0.23$; *m*AHP, $t_{(4)} = 0.54$, $p = 0.62$) (Fig. 7*H–J*) or evoked action potential firing ($F_{(1,56)} = 0.07$, $p = 0.79$) (Fig. 7*K*). Thus, it was likely that the expression of SK channels was minimal in NAc MSNs not expressing *h*SMP. In contrast, in NAc MSNs expressing DCS-induced *h*SMP, application of apamin completely restored the frequency of action potential firing to the control level ($F_{(2,352)} = 34.6$, $p < 0.01$; posttest, $p = 1.00$, control vs DCS + apamin) (Fig. 7*L*). Furthermore, these *h*SMP-expressing MSNs exhibited a significant increase in *m*AHP, and the increased portion of *m*AHP was completely abolished by application of apamin ($F_{(2,33)} = 5.37$, $p < 0.01$; posttest, $p = 0.66$, control vs DCS + apamin) (Fig. 7*M*,*N*). The appearance of apamin-sensitive *m*AHP following DCS-treatment indicated that either new SK channels were expressed or the existing but latent SK channels were activated. Thus, modification of SK channels likely serve as one of the key mechanisms underlying the expression of *h*SMP.

Implication of *h*SMP in cocaine-induced membrane adaptation

Finally, we explored the role of *h*SMP in drug-induced functional alterations of NAc MSNs. It has been shown that withdrawal from repeated exposure to cocaine increases the excitatory synaptic strength (Churchill et al., 1999; Kourrich et al., 2007; Conrad et al., 2008) as well as decreases the intrinsic membrane excitability (Dong et al., 2006) of NAc MSNs. To determine whether *h*SMP is implicated in these concurrent synaptic and membrane changes following cocaine administration, we examined *h*SMP in NAc MSNs following repeated cocaine exposure.

We first examined rats treated with the 5 d cocaine procedure, followed by a 2 d withdrawal. Consistent with previous results (Dong et al., 2006), the basal membrane excitability of NAc MSNs in cocaine-treated rats was significantly decreased, and the effect of cocaine was more pronounced upon higher injected currents ($F_{(3,352)} = 3.80$, treatment × current injection; $p < 0.05$ at 150–400 pA). Furthermore, incubation of DCS no longer induced *h*SMP in NAc MSNs from cocaine-treated rats ($F_{(3,352)} = 36.3$, $p < 0.01$; posttest, $p = 1.00$, cocaine-control vs cocaine-DCS) (Fig. 8*A*). Concurrent with the cocaine-induced decrease in action potential firing, the *m*AHP ($F_{(3,44)} = 5.82$, $p < 0.01$), but not *f*AHP ($F_{(3,44)} = 0.78$, $p = 0.51$), was also increased with a pattern similar to that observed in NAc MSNs after DCS-induced *h*SMP (Fig. 8*B*,*C*). These results raise a possibility that the cocaine-induced decrease in membrane excitability of NAc MSNs is mediated by *h*SMP, as a consequence of increased excitatory synaptic input. If this is the case, inhibiting the *m*AHP with apamin, which prevented *h*SMP-mediated modulation of membrane excitability, should abolish the effect of cocaine on the membrane excitability of NAc MSNs. To explore this possibility, we incubated the acutely prepared slices with apamin (300 nM, no incubation as a control) from cocaine-pretreated rats (saline-pretreated rats as controls) and observed that incubation of apamin partially reversed the cocaine-induced decrease in evoked action potential firing in NAc MSNs ($F_{(3,256)} = 17.4$, $p < 0.01$; posttest, $p < 0.01$, cocaine vs cocaine + apamin; $p = 0.48$, saline + apamin vs cocaine + apamin) (Fig. 8*D*). Partial, rather than complete, restoration of the membrane excitability by apamin suggest that (1) the *m*AHP-based mechanism of *h*SMP may mediate in part cocaine-induced decrease in the membrane excitability of NAc MSNs; and (2) other mechanisms independent of *m*AHP are also involved in the effect of cocaine on membrane excitability of NAc MSNs.

To understand *h*SMP as well as the effect of cocaine on membrane excitability of NAc MSNs in a longer withdrawal period, we next examined the rats with the same 5 d cocaine procedure, followed by a 3 week withdrawal. Accordingly, rats used in this set of experiments were 3 weeks older than those used in the 2 d withdrawal experiments. It has been shown that the frequency of evoked action potential firing gradually decreases when the ani-

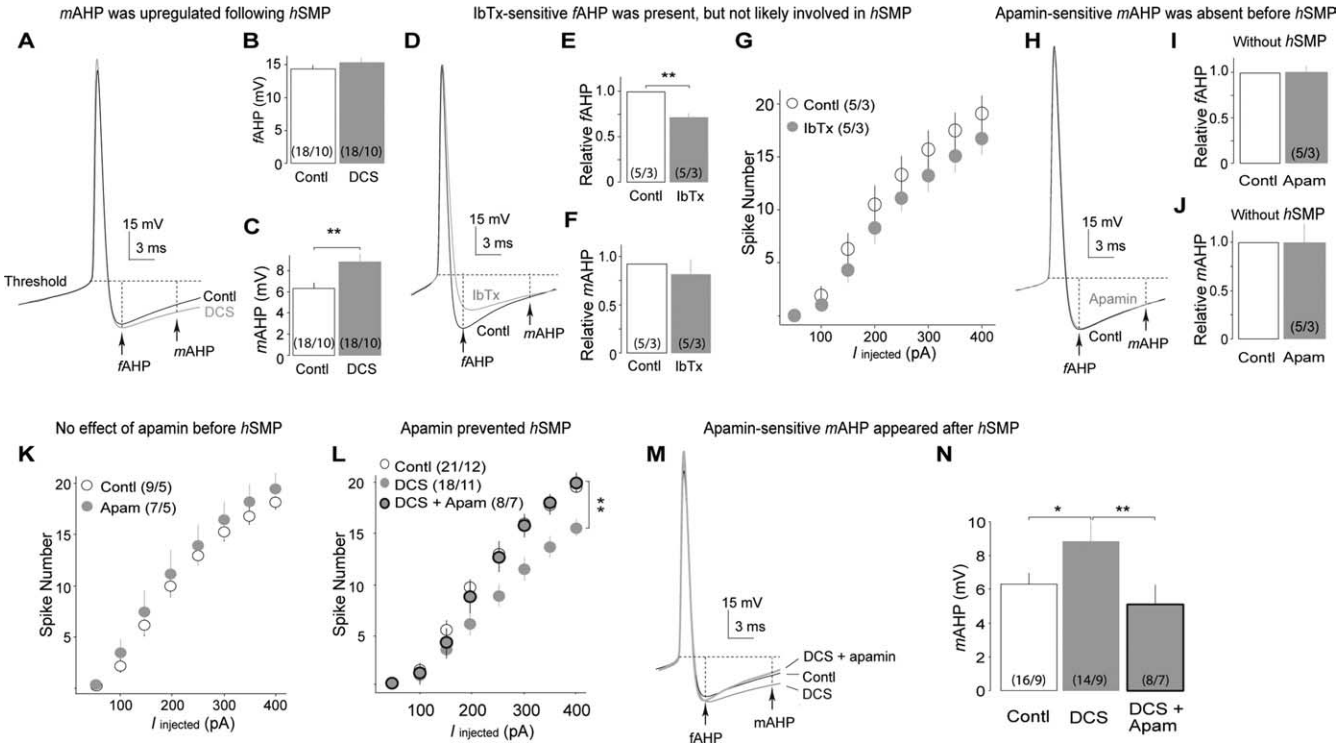

Figure 7. Calcium-activated SK potassium channels as the expression substrates of *h*SMP in NAc MSNs. ***A***, Averaged AHP traces from 21 control NAc MSNs (black) and 18 MSNs expressing DCS-induced *h*SMP (gray). ***B***, ***C***, Summaries showing that the *m*AHP (***C***), but not *f*AHP (***B***), was increased in *h*SMP-expressing NAc MSNs. ***D***, Averaged AHP traces from 5 NAc MSNs before (black) and after (gray) application of BK channel-selective antagonist iberiotoxin (IbTx, 100 nM). ***E***, ***F***, Summaries showing that *f*AHP, but not *m*AHP, was significantly decreased by inhibition of BK channels. ***G***, A summary showing that inhibition of BK channels did not significantly alter the action potential firing in NAc MSNs. ***H***, Averaged AHP traces from 5 NAc MSNs before (black) and after (gray) application of SK channel selective antagonist apamin (300 nM). ***I***, ***J***, Summaries showing that no effect of apamin on *f*/*m*AHP and, thus, no SK channel activities were detected in control NAc MSNs. ***K***, A summary showing that application of apamin did not affect action potential firing in control NAc MSNs. ***L***, A summary showing that coincubation of apamin prevented the DCS-induced *h*SMP in NAc MSNs. ***M***, Averaged AHP traces from 16 control NAc MSNs, 14 MSNs treated with DCS, and 8 MSNs treated with DCS and apamin. ***N***, A summary showing that 5 h incubation of DCS selectively increased the *m*AHP component in NAc MSNs, an effect that could be reversed by additional application of apamin. *$p < 0.05$; **$p < 0.01$; (*n*/*m*), number of cells/number of animals.

mal becomes older (Tombaugh et al., 2005; Frick et al., 2007; Yan et al., 2009). This is also true for NAc MSNs (see supplemental material, available at www.jneurosci.org). To minimize this age-dependent variation, we performed this experiment using a set of age-matched rats (at postnatal 54–56 d on the recording day). Following 3 weeks of withdrawal from cocaine administration, the membrane excitability of NAc MSNs remained at a low level, and incubation of DCS did not induce *h*SMP in NAc MSNs from cocaine-pretreated rats ($F_{(3,320)} = 8.52$, $p < 0.01$) (Fig. 8*E*).

One related issue is that the rats used in these experiments were immediately placed back to their home cages after the cocaine injections. Thus, the potential context-related enhancement of the drug effect may not be detected (Badiani et al., 1997). Nonetheless, the above results suggest that *h*SMP in NAc MSNs is either disabled or already saturated in cocaine-treated rats during short- or long-term withdrawal.

Discussion

Using both cultured and acute NAc slices, we demonstrated *h*SMP, which was initiated by synaptic NMDARs and expressed, in part, by modulation of SK type calcium-activated potassium channels. This *h*SMP may represent a novel mechanism that balances the synaptic input and membrane excitability to achieve neuronal homeostasis.

Homeostatic synapse–membrane cross talk

The membrane excitability and synaptic input are two key determinants that set the functional output of a neuron. Homeostatic mechanisms exist for excitatory synapses or membrane excitability in a relatively independent manner (Turrigiano and Nelson, 2004). However, to achieve the overall stability of the entire neuron, higher orders of homeostatic mechanisms must exist to coordinate the synaptic activity and membrane excitability. Such synapse–membrane homeostatic plasticity was reported in cultured lobster stomatogastric ganglion neurons, in which the synapse-induced rhythmic oscillation of membrane potential was lost by removal of excitatory synapses but subsequently restored by homeostatic changes in the membrane properties (Turrigiano et al., 1994). However, homeostatic synapse–membrane crosstalk has not been well understood in mammalian central neurons, which possess more complicated input–output regulations (Destexhe and Marder, 2004).

*h*SMP as presently identified in the NAc may serve as a potentially common homeostatic mechanism in the mammalian central neurons that coordinates synaptic input and membrane excitability to achieve a functional stability at the whole-cell level. This stability-maintaining feature of *h*SMP can be largely exemplified in the *in vivo* NAc MSNs. In the *in vivo* NAc MSNs, the membrane potential oscillates between two excitable states (O'Donnell and Grace, 1995; Mahon et al., 2006). One is called the down state, during which the MSNs rest at a hyperpolarized potential (approximately −78 mV) and remain largely quiescent. The other is called the up state, which is the functional active state during which the MSNs dwell at a less negative plateau potential (approximately −55 mV) and are apt to fire action potentials.

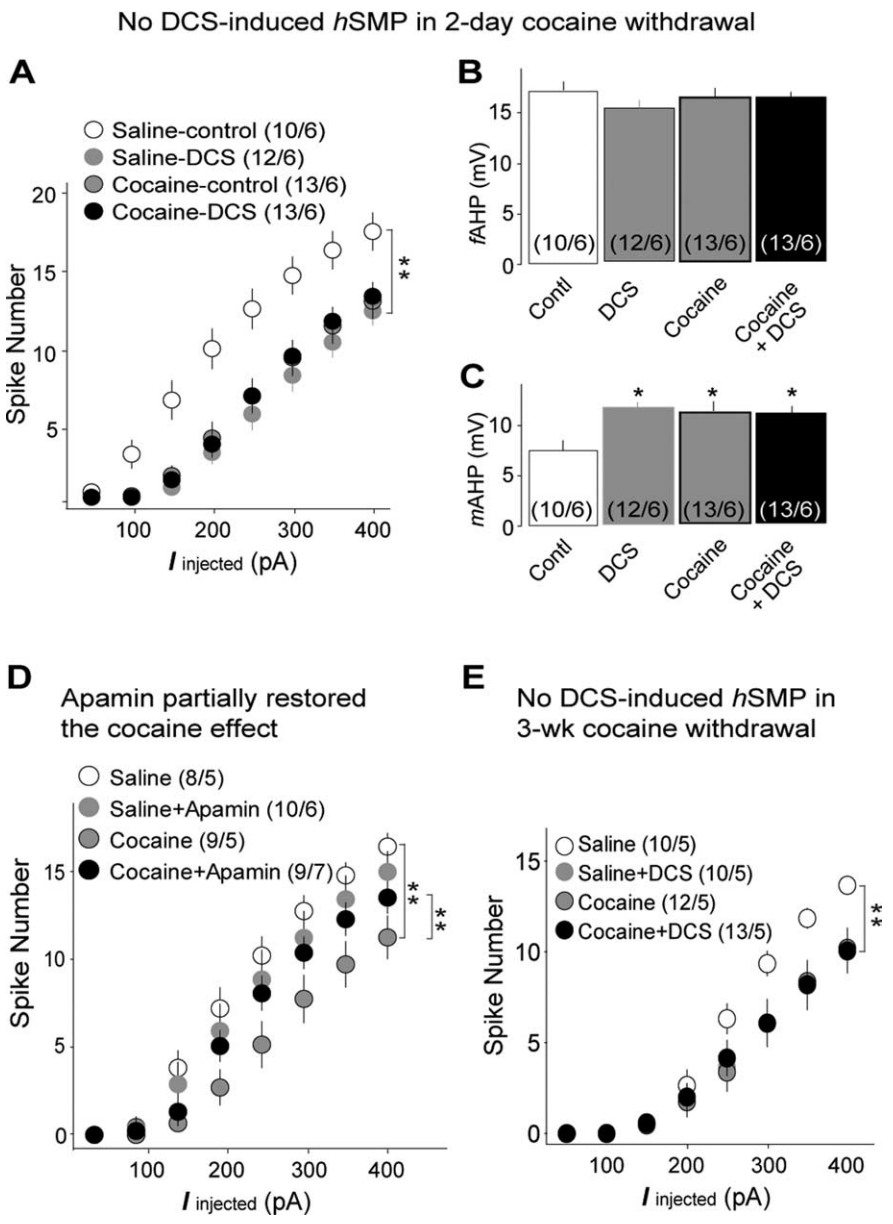

Figure 8. NAc *h*SMP in cocaine-treated rats. ***A***, Summarized results showing that 2 d withdrawal from 5 d cocaine administration decreased the membrane excitability of NAc MSNs. Incubation of DCS did not further decrease the membrane excitability of NAc MSNs from cocaine-treated rats. ***B***, ***C***, Summarized results showing that *m*AHP, but not *f*AHP, was concurrently increased in NAc MSNs in which the membrane excitability was decreased following 2 d withdrawal from repeated cocaine administration. ***D***, Summarized results showing that inhibiting *m*AHP partially restored the membrane excitability of NAc MSNs from cocaine-pretreated rats (with 2 d withdrawal). ***E***, Summarized results showing that following 3 week withdrawal from repeated cocaine administration, the membrane excitability of NAc MSNs remained low. Incubation of DCS did not further decrease the membrane excitability of these neurons. $*p < 0.05$; (*n*/*m*), number of cells/number of animals.

*h*SMP can also be important in maintaining interneuronal stability. Within the neural circuit, the intensity of synaptic input reflects the activity state of the networked neurons. Thus, via *h*SMP, neurons can continuously adjust their membrane excitability to contribute to the overall stability of the neural circuit. Furthermore, our results show that this synapse–membrane homeostatic crosstalk can be initiated by the D-serine binding site of NMDARs. Because D-serine is primarily released by glial cells, this *h*SMP may also mediate important glia-neuron homeostatic interactions.

BK and SK channels

Calcium-activated BK and SK potassium channels hyperpolarize the membrane potential after the action potential and, thus, often effectively inhibit generation of the subsequent action potentials. However, BK channels also contribute to the post-action potential repolarization, which expedite the recovery of the neuron for the subsequent action potential. Thus, the overall effect of BK channels on membrane excitability can be either "excitatory" or "inhibitory" depending on their subunit composition and posttranslational regulations (Stocker, 2004). The "excitatory" effect of BK channels may underlie the minimal (not significant) inhibition of action potential firing by IbTx (Fig. 7*G*). Nonetheless, it appears that BK channels are not preferentially involved in the expression of *h*SMP in NAc MSNs (Fig. 7*A–F*).

In contrast, SK channels are critical for expressing *h*SMP in NAc MSNs (Fig. 7*L–N*). Due to the relatively slow activation and inactivation kinetics, SK channels are primarily inhibitory on repetitive action potential firing. Because SK channels are activated upon action potential-induced Ca^{2+} influx, a high activity level (more action potential firing) of a neuron is, in theory, accompanied by a high level of activation of SK channels and, thus, a high level of SK channel-mediated inhibition. Thus, this SK channel-based negative feedback loop per se is, to some extent, homeostatic. However, this potential feedback loop appears not to preexist in NAc shell MSNs because no significant SK channel activity was detected at 3 h *in vitro* (Fig. 7*H–J*). In contrast, a significant level of SK channel activity appeared in MSNs expressing *h*SMP (Fig. 7*M*,*N*). Two possible mechanisms may underlie this *h*SMP-associated functional expression of SK channels. One is that SK channels, indeed, exist on the membrane of NAc MSNs but are maximally inhibited by the external (Lu et al., 2000) or internal (Fanger et al., 1999) regulators; continuous activation of NMDAR signaling removes these inhibitions and SK channels become functionally active. Another possibility is that SK channels do not preexist on the

The up state potential plateau of NAc MSNs is initiated/maintained by synchronized glutamatergic inputs (Wilson, 1986; Plenz and Kitai, 1998; O'Donnell et al., 1999). Whereas the up state brings the membrane toward the threshold of action potential firing, the intrinsic membrane excitability determines whether and how often to fire action potentials during the up state. As such, when a pathological insult increases the excitatory synaptic inputs to NAc MSNs and, thus, increases the duration of the up state, if *h*SMP functions effectively to decrease the intrinsic membrane excitability, NAc MSNs may still be able to fire the same number of action potentials and, thus, maintain relatively normal functional output.

membrane whereas continuous activation of NMDAR signaling induces a quick surface expression of these channels. Along this line, it has been shown that assembly and surface expression of SK channels are dynamically regulated by a variety of intracellular signaling proteins (Wei et al., 2000; Stocker, 2004; Ren et al., 2006). Nonetheless, our data suggest that a dynamic change in the function/number of surface SK channels mediates one direction (depression of membrane excitability) of *h*SMP in NAc MSNs. The lack of basal activity of SK channels (Fig. 7*H–J*) suggests that a SK channel-independent mechanism is involved in the other direction of *h*SMP.

Potential role of *h*SMP in cocaine-induced plasticity in the NAc

Cocaine-induced functional alterations of the NAc contribute to cocaine-elicited behavioral alterations (Wolf et al., 2004; Kalivas, 2005; Shaham and Hope, 2005; Vezina, 2007). As such, the effects of cocaine on synaptic input and intrinsic membrane excitability of NAc MSNs, the two major determinants of the functional output of neurons, have been extensively examined. The available results together with our present findings suggest that *h*SMP may be involved in some, but not all phases of cocaine-induced synaptic and membrane adaptations in the NAc MSNs. During short-term (1 d) withdrawal from repeated intraperitoneal injections of cocaine or cocaine self administration, both the surface (Boudreau and Wolf, 2005; Conrad et al., 2008) and total (Churchill et al., 1999) levels of AMPAR subunits remain unchanged in the NAc. At a similar time point, the AMPAR/NMDAR ratio at excitatory synapses of NAc MSNs is decreased, which was interpreted as a decrease in the number/function of AMPARs (Kourrich et al., 2007). This interpretation is consistent with the observations that following cocaine exposure the *in vivo* NAc MSNs become less responsive to iontophoretic glutamate (White et al., 1995) and the LTD of excitatory synaptic transmission to NAc MSNs appears to be saturated (Martin et al., 2006). Despite the synaptic AMPARs being unchanged or decreased, the intrinsic membrane excitability of NAc MSNs is decreased during short-term withdrawal (Dong et al., 2006). Therefore, the decrease in membrane excitability should be primarily mediated by other mechanisms instead of *h*SMP, unless there are changes in synaptic NMDARs. Previous studies did not detect changes in NMDARs in fully functional/nonsilent synapses in NAc MSNs (Kourrich et al., 2007). However, NMDARs within the potential silent synapses (Thomas et al., 2001) may be enhanced to induce an *h*SMP-mediated decrease in the membrane excitability of NAc MSNs.

During long-term (>10 d) withdrawal from repeated intraperitoneal injections of cocaine or cocaine self administration, both the surface and total levels of AMPAR subunits are increased in NAc MSNs (Churchill et al., 1999; Boudreau and Wolf, 2005; Boudreau et al., 2007; Conrad et al., 2008). At a similar time point, the AMPAR/NMDAR ratio of NAc MSNs is also increased (Kourrich et al., 2007). In addition, both the surface level of AMPAR subunits and the AMPAR/NMDAR ratio are rapidly decreased upon a reexposure to cocaine during long-term withdrawal (Boudreau et al., 2007; Kourrich et al., 2007). On the other hand, the intrinsic membrane excitability of NAc MSNs remains low during long-term withdrawal from cocaine administration (Fig. 8). Thus, during long-term withdrawal, changes in excitatory synapses and membrane excitability of NAc MSNs are, to some degree, homeostatically cancelled at the functional level. The observations that *h*SMP is abolished and the SK channels are upregulated when taken together suggest that the *h*SMP-related mechanisms are involved in regulating the membrane excitability of NAc MSNs during withdrawal from cocaine administration.

Whereas identification of *h*SMP provides a novel angle to understand cocaine-induced plastic changes, it should be noted that other plasticity mechanisms, such as experience-dependent, or Hebbian, plasticity are also important in reshaping the cellular properties of NAc MSNs following exposure to cocaine (Hyman et al., 2006). Thus, the "final" drug-induced plastic changes observed in the NAc should result from the interaction between homeostatic, Hebbian, and other forms of plasticity.

References

Aizenman CD, Linden DJ (2000) Rapid, synaptically driven increases in the intrinsic excitability of cerebellar deep nuclear neurons. Nat Neurosci 3:109–111.

Badiani A, Camp DM, Robinson TE (1997) Enduring enhancement of amphetamine sensitization by drug-associated environmental stimuli. J Pharmacol Exp Ther 282:787–794.

Boudreau AC, Wolf ME (2005) Behavioral sensitization to cocaine is associated with increased AMPA receptor surface expression in the nucleus accumbens. J Neurosci 25:9144–9151.

Boudreau AC, Reimers JM, Milovanovic M, Wolf ME (2007) Cell surface AMPA receptors in the rat nucleus accumbens increase during cocaine withdrawal but internalize after cocaine challenge in association with altered activation of mitogen-activated protein kinases. J Neurosci 27:10621–10635.

Cavelier P, Attwell D (2007) Neurotransmitter depletion by bafilomycin is promoted by vesicle turnover. Neurosci Lett 412:95–100.

Chang CP, Dworetzky SI, Wang J, Goldstein ME (1997) Differential expression of the alpha and beta subunits of the large-conductance calcium-activated potassium channel: implication for channel diversity. Brain Res Mol Brain Res 45:33–40.

Churchill L, Swanson CJ, Urbina M, Kalivas PW (1999) Repeated cocaine alters glutamate receptor subunit levels in the nucleus accumbens and ventral tegmental area of rats that develop behavioral sensitization. J Neurochem 72:2397–2403.

Conrad KL, Tseng KY, Uejima JL, Reimers JM, Heng LJ, Shaham Y, Marinelli M, Wolf ME (2008) Formation of accumbens GluR2-lacking AMPA receptors mediates incubation of cocaine craving. Nature 454:118–121.

Davis GW (2006) Homeostatic control of neural activity: from phenomenology to molecular design. Annu Rev Neurosci 29:307–323.

Desai NS, Rutherford LC, Turrigiano GG (1999) Plasticity in the intrinsic excitability of cortical pyramidal neurons. Nat Neurosci 2:515–520.

Destexhe A, Marder E (2004) Plasticity in single neuron and circuit computations. Nature 431:789–795.

Dong Y, Saal D, Thomas M, Faust R, Bonci A, Robinson T, Malenka RC (2004) Cocaine-induced potentiation of synaptic strength in dopamine neurons: behavioral correlates in GluRA(-/-) mice. Proc Natl Acad Sci U S A 101:14282–14287.

Dong Y, Nasif FJ, Tsui JJ, Ju WY, Cooper DC, Hu XT, Malenka RC, White FJ (2005) Cocaine-induced plasticity of intrinsic membrane properties in prefrontal cortex pyramidal neurons: adaptations in potassium currents. J Neurosci 25:936–940.

Dong Y, Green T, Saal D, Marie H, Neve R, Nestler EJ, Malenka RC (2006) CREB modulates excitability of nucleus accumbens neurons. Nat Neurosci 9:475–477.

Egorov AV, Hamam BN, Fransén E, Hasselmo ME, Alonso AA (2002) Graded persistent activity in entorhinal cortex neurons. Nature 420:173–178.

Fanger CM, Ghanshani S, Logsdon NJ, Rauer H, Kalman K, Zhou J, Beckingham K, Chandy KG, Cahalan MD, Aiyar J (1999) Calmodulin mediates calcium-dependent activation of the intermediate conductance KCa channel, IKCa1. J Biol Chem 274:5746–5754.

Frick A, Feldmeyer D, Sakmann B (2007) Postnatal development of synaptic transmission in local networks of L5A pyramidal neurons in rat somatosensory cortex. J Physiol 585:103–116.

Huang YH, Lin Y, Brown TE, Han MH, Saal DB, Neve RL, Zukin RS, Sorg BA, Nestler EJ, Malenka RC, Dong Y (2008) CREB modulates the functional output of nucleus accumbens neurons: a critical role of *N*-methyl-D-aspartate glutamate receptor (NMDAR) receptors. J Biol Chem 283:2751–2760.

Hyman SE, Malenka RC, Nestler EJ (2006) Neural mechanisms of addiction: the role of reward-related learning and memory. Annu Rev Neurosci 29:565–598.

Ibata K, Sun Q, Turrigiano GG (2008) Rapid synaptic scaling induced by changes in postsynaptic firing. Neuron 57:819–826.

Jahr CE, Stevens CF (1990) Voltage dependence of NMDA-activated macroscopic conductances predicted by single-channel kinetics. J Neurosci 10:3178–3182.

Kalivas PW (2005) How do we determine which drug-induced neuroplastic changes are important? Nat Neurosci 8:1440–1441.

Kelley AE (2004) Ventral striatal control of appetitive motivation: role in ingestive behavior and reward-related learning. Neurosci Biobehav Rev 27:765–776.

Kourrich S, Rothwell PE, Klug JR, Thomas MJ (2007) Cocaine experience controls bidirectional synaptic plasticity in the nucleus accumbens. J Neurosci 27:7921–7928.

Lee BR, Mu P, Saal DB, Ulibarri C, Dong Y (2008) Homeostatic recovery of downstate-upstate cycling in nucleus accumbens neurons. Neurosci Lett 434:282–288.

Lois C, Hong EJ, Pease S, Brown EJ, Baltimore D (2002) Germline transmission and tissue-specific expression of transgenes delivered by lentiviral vectors. Science 295:868–872.

Lu M, MacGregor GG, Wang W, Giebisch G (2000) Extracellular ATP inhibits the small-conductance K channel on the apical membrane of the cortical collecting duct from mouse kidney. J Gen Physiol 116:299–310.

Mahon S, Vautrelle N, Pezard L, Slaght SJ, Deniau JM, Chouvet G, Charpier S (2006) Distinct patterns of striatal medium spiny neuron activity during the natural sleep-wake cycle. J Neurosci 26:12587–12595.

Malenka RC, Nicoll RA (1999) Long-term potentiation—a decade of progress? Science 285:1870–1874.

Marie H, Morishita W, Yu X, Calakos N, Malenka RC (2005) Generation of silent synapses by acute in vivo expression of CaMKIV and CREB. Neuron 45:741–752.

Martin M, Chen BT, Hopf FW, Bowers MS, Bonci A (2006) Cocaine self-administration selectively abolishes LTD in the core of the nucleus accumbens. Nat Neurosci 9:868–869.

Nelson AB, Krispel CM, Sekirnjak C, du Lac S (2003) Long-lasting increases in intrinsic excitability triggered by inhibition. Neuron 40:609–620.

O'Donnell P, Grace AA (1995) Synaptic interactions among excitatory afferents to nucleus accumbens neurons: hippocampal gating of prefrontal cortical input. J Neurosci 15:3622–3639.

O'Donnell P, Greene J, Pabello N, Lewis BL, Grace AA (1999) Modulation of cell firing in the nucleus accumbens. Ann N Y Acad Sci 877:157–175.

Plenz D, Kitai ST (1998) Up and down states in striatal medium spiny neurons simultaneously recorded with spontaneous activity in fast-spiking interneurons studied in cortex-striatum-substantia nigra organotypic cultures. J Neurosci 18:266–283.

Ren Y, Barnwell LF, Alexander JC, Lubin FD, Adelman JP, Pfaffinger PJ, Schrader LA, Anderson AE (2006) Regulation of surface localization of the small conductance Ca2+-activated potassium channel, Sk2, through direct phosphorylation by cAMP-dependent protein kinase. J Biol Chem 281:11769–11779.

Saal D, Dong Y, Bonci A, Malenka RC (2003) Drugs of abuse and stress trigger a common synaptic adaptation in dopamine neurons. Neuron 37:577–582.

Sailer CA, Hu H, Kaufmann WA, Trieb M, Schwarzer C, Storm JF, Knaus HG (2002) Regional differences in distribution and functional expression of small-conductance Ca2+-activated K+ channels in rat brain. J Neurosci 22:9698–9707.

Schlüter OM, Xu W, Malenka RC (2006) Alternative N-terminal domains of PSD-95 and SAP97 govern activity-dependent regulation of synaptic AMPA receptor function. Neuron 51:99–111.

Shaham Y, Hope BT (2005) The role of neuroadaptations in relapse to drug seeking. Nat Neurosci 8:1437–1439.

Sourdet V, Russier M, Daoudal G, Ankri N, Debanne D (2003) Long-term enhancement of neuronal excitability and temporal fidelity mediated by metabotropic glutamate receptor subtype 5. J Neurosci 23:10238–10248.

Stocker M (2004) Ca(2+)-activated K+ channels: molecular determinants and function of the SK family. Nat Rev Neurosci 5:758–770.

Thomas MJ, Beurrier C, Bonci A, Malenka RC (2001) Long-term depression in the nucleus accumbens: a neural correlate of behavioral sensitization to cocaine. Nat Neurosci 4:1217–1223.

Tombaugh GC, Rowe WB, Rose GM (2005) The slow afterhyperpolarization in hippocampal CA1 neurons covaries with spatial learning ability in aged Fisher 344 rats. J Neurosci 25:2609–2616.

Turrigiano G, Abbott LF, Marder E (1994) Activity-dependent changes in the intrinsic properties of cultured neurons. Science 264:974–977.

Turrigiano GG, Nelson SB (2004) Homeostatic plasticity in the developing nervous system. Nat Rev Neurosci 5:97–107.

Vezina P (2007) Sensitization, drug addiction and psychopathology in animals and humans. Prog Neuropsychopharmacol Biol Psychiatry 31:1553–1555.

Wei Y, Bloom P, Gu R, Wang W (2000) Protein-tyrosine phosphatase reduces the number of apical small conductance K+ channels in the rat cortical collecting duct. J Biol Chem 275:20502–20507.

White FJ, Hu XT, Zhang XF, Wolf ME (1995) Repeated administration of cocaine or amphetamine alters neuronal responses to glutamate in the mesoaccumbens dopamine system. J Pharmacol Exp Ther 273:445–454.

Wilson CJ (1986) Postsynaptic potentials evoked in spiny neostriatal projection neurons by stimulation of ipsilateral and contralateral neocortex. Brain Res 367:201–213.

Wilson CJ, Groves PM (1980) Fine structure and synaptic connections of the common spiny neuron of the rat neostriatum: a study employing intracellular inject of horseradish peroxidase. J Comp Neurol 194:599–615.

Wilson CJ, Kawaguchi Y (1996) The origins of two-state spontaneous membrane potential fluctuations of neostriatal spiny neurons. J Neurosci 16:2397–2410.

Wolf ME, Sun X, Mangiavacchi S, Chao SZ (2004) Psychomotor stimulants and neuronal plasticity. Neuropharmacology 47 Suppl 1:61–79.

Xu J, Kang J (2005) The mechanisms and functions of activity-dependent long-term potentiation of intrinsic excitability. Rev Neurosci 16:311–323.

Xu J, Kang N, Jiang L, Nedergaard M, Kang J (2005) Activity-dependent long-term potentiation of intrinsic excitability in hippocampal CA1 pyramidal neurons. J Neurosci 25:1750–1760.

Yan H, Li Q, Fleming R, Madison RD, Wilson WA, Swartzwelder HS (2009) Developmental sensitivity of hippocampal interneurons to ethanol: involvement of the hyperpolarization-activated current, Ih. J Neurophysiol 101:67–83.

Zhang W, Linden DJ (2003) The other side of the engram: experience-driven changes in neuronal intrinsic excitability. Nat Rev Neurosci 4:885–900.

Zhou Q, Petersen CC, Nicoll RA (2000) Effects of reduced vesicular filling on synaptic transmission in rat hippocampal neurones. J Physiol 525:195–206.

Ziskin JL, Nishiyama A, Rubio M, Fukaya M, Bergles DE (2007) Vesicular release of glutamate from unmyelinated axons in white matter. Nat Neurosci 10:321–330.